

BACKGROUND

Understanding response to immunotherapy requires accurate and complete characterization of tumor-associated immune cells in order to fully contextualize the immuno-oncology biomarker expression. Current standard practices surrounding enumeration of biomarker-positive immune cells using image analysis necessitate a dual-labeling approach combining the biomarker of interest and immune cell identification assays.

Machine Learning (ML) may be used to distinguish different tissue types in a biopsy (e.g. tumor vs. non-tumor), or to identify different cell types (e.g. macrophages vs other cells). A ML algorithm obtains statistics for a specific tissue class or cell type based on a training set, given by "ground truth" examples. The algorithm then generalizes from the given examples to "learn" the ability to find the tissue or cell type on the rest of the digital scan of the tissue slide, or other scans.

Here we specifically describe ML methods for macrophage identification in digital scans of non-small cell lung carcinoma (NSCLC) tissue slides. In Method 1, the ML algorithm was trained by pathologist assistance. In Method 2, the ML algorithm was trained by immunofluorescence assistance. While both methods enable quantification of macrophages without the routine use of immunohistochemistry (IHC) to label the macrophages, the two methods are distinct and will be described separately.

METHOD 1

Methods All stained NSCLC samples were annotated for a region of analysis (ROA) and training annotations were placed by a pathologist for macrophage and non-macrophage cells including tumor, stroma, and immune cells. Macrophages were identified and annotated by the pathologist as the "ground truth" by using morphological features of macrophages that are previously described. The number of cells in each training annotation ranged from 1 cell to up to 25-50 cells in a cluster. Training annotations were utilized by Flagship's proprietary computational Tissue Analysis (cTA) software to enable the use of ML to classify all cells present in the ROA. Once all cells were classified by cTA ML, the results were qualitatively reviewed for the accuracy of classification by an MD board-certified pathologist. The number of cells classified as macrophages and non-macrophages was also quantified.

Results A total of 20 NSCLC samples were used for testing this method. Macrophages were identified by the pathologist with confidence in 14 out of 20 cases (70%). Out of the 14 cases, the ML classification of macrophages in the entire ROA worked on 6 cases (Table 1). Overall these data represent a success rate of approximately 30% for the ability to adequately train the cTA algorithm for macrophage identification. However, among the cells identified by the trained ML algorithm, pathologist review determined the accuracy of proper classification only ranged from 1-25%. Of note, the majority of the morphologically identified macrophages were alveolar macrophages; most of the misclassification by the cTA ML process occurred by tumor cells being misclassified as macrophages. Figure 1 shows some example markups of cTA detection of macrophages after pathologist-training of the algorithm.

Table 1. Identification of Macrophages Using Pathologist-Assisted ML Training

Sample ID	Macrophages		Non-macrophages		Total Cell #	Accuracy
	#	%	#	%		
NSCLC 20	29282	4.2%	661820	95.8%	691102	25
NSCLC 58	6498	1.0%	632469	99.0%	638967	1
NSCLC 76	7378	5.8%	120348	94.2%	127726	5
NSCLC 95	112668	9.1%	1121843	90.9%	1234511	1
NSCLC 101	37312	10.2%	330086	89.8%	367398	1
NSCLC 125	162191	14.8%	933704	85.2%	1095895	20

METHOD 2

Methods 15 NSCLC and 1 tonsil tissue sections were dual-stained for CD68 (by immunofluorescence, IF) and for PD-L1 (by IHC). Brightfield and IF scans were co-registered using the nuclear identifying channels (Hematoxylin and DAPI), and the images were overlaid. CD68 staining was then used as the "ground truth" to automatically select macrophages in the brightfield scan without affecting the brightfield image. This approach enabled training of a ML classifier that was capable of recognizing macrophages in the absence of a macrophage-specific IHC stain. After the cTA ML classifier was applied to the ROA, the number of macrophages vs. total cells present in the ROA was determined for each sample, and the presence of CD68 staining in macrophages identified by the cTA ML classifier was also evaluated. In addition, the macrophages identified by CD68 staining in each section was quantified using the IF image only. A confusion matrix was generated for comparison of the macrophages identified by cTA ML vs. those identified by CD68 staining alone.

Results Confusion matrices were run for every sample analyzed to compare the Brightfield cTA ML detection of macrophages to the IF CD68 detection of macrophages. Table 2 shows an overall confusion matrix as a comprehensive total of all macrophages identified across all samples by either cTA ML or CD68. The overall accuracy of the cTA ML detection was 74.85%. Figure 2 shows a series of images to demonstrate each stage of the process from a single sample.

Table 2. Confusion Matrix Comparing Identification of Macrophages Using Immunofluorescence-Assisted ML Training vs. CD68 Staining

Sample ID	Total Cell Number Identified As:		Accuracy (%)	False Positives Rate	False Negatives Rate
	CD68+	CD68-			
ML classifier	349899	1542742	74.85	20.62	4.54
CD68 IF Staining	339621	5251187			

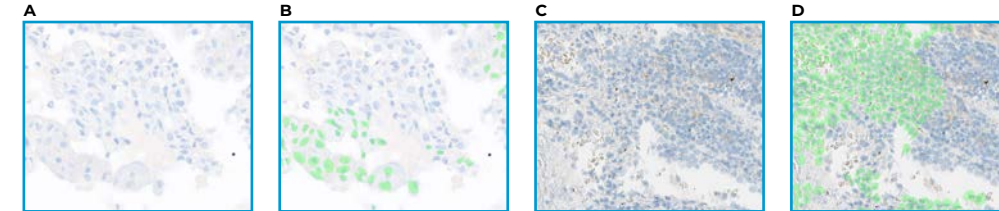


Figure 1. Macrophage Detection Using Pathologist-Assisted ML Training. Using macrophage-specific morphologic features, the ML cTA algorithm was trained sample-by-sample by an MD board-certified anatomic pathologist. The trained ML algorithm was applied to the entire ROA and example images are shown here. (A & B) IHC image (A) and cTA ML marking of macrophages identified by ML (B) for sample NSCLC 101. The region shown demonstrates appropriate classification. (C & D) IHC image (C) and cTA ML marking of macrophages identified by ML (D) for sample NSCLC 95. The region shown demonstrates inappropriate classification. (B & D) Cells highlighted in green are classified as macrophages by the trained cTA ML algorithm.

Discussion Alveolar macrophages were relatively easy for the pathologist to identify and use to train the cTA algorithm. Overall, however, training the cTA algorithm using pathologist-identified macrophages is challenging given the difficulty in morphologically identifying all macrophages, especially tissue macrophages. Furthermore, there is a very limited number of collections of pure macrophages without intermixed non-macrophage-like cells. Flagship regularly utilizes pathologist-assisted ML to segregate cells into the tumor and tumor microenvironment (TME) compartments with great success. For subclassifying TME cells such as macrophages, however, it has been concluded that using a pathologist-assisted, morphology-based training may not be an ideal method to train cTA ML for successful cell identification.

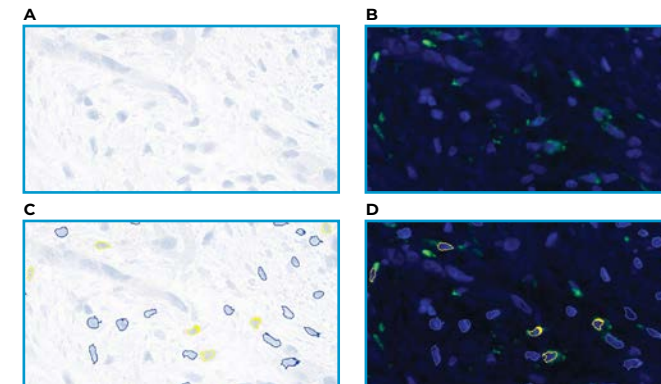


Figure 2. Macrophage Detection Using Immunofluorescence-Assisted ML Training. (A) IHC Brightfield image before cTA ML training. Blue staining is hematoxylin. (B) IF image used for cTA ML training. Blue staining is DAPI, green staining is the FITC channel for detection of CD68. (C) Brightfield image after cTA ML training. Blue outline denotes cells classified as macrophages after the trained cTA ML classifier was applied to the whole ROA. Yellow outline denotes cells that are identified as macrophages that are also CD68-positive when comparing the detected cell back to the IF image. Blue staining is hematoxylin. (D) IF image showing the results of the cTA ML training applied back to the IF image. Blue outline denotes cells classified as macrophages after the trained cTA ML classifier was applied to the whole ROA. Yellow outline denotes cells that were identified as macrophages that were also CD68-positive when comparing the detected cell back to the IF image. Blue staining is DAPI, green staining is the FITC channel for detection of CD68.

Discussion Training the cTA algorithm with the immunofluorescent image assistance identifies macrophages in tissue sections. The increased presence of CD68 staining in the cTA ML detected macrophages demonstrates the algorithms' ability to identify a population likely to be macrophages. However, comparison to the CD68 IF image and quantification suggests that further refinement of this process is necessary to improve specificity. The application of this method to PD-L1 stained sections (or any IHC assay stained sections) could help identify the staining pattern of specific cell types in both tumor and TME tissue compartments. Generalization of this process to other immune cell subsets may lead to the better characterization of the immune landscape in tumor samples, eliminating the need for additional IHC to characterize specific cells.

CONCLUSIONS

Here we present two unique methods to detect macrophages in an IHC-stained tissue section in the absence of a macrophage-specific IHC stain.

Method 1, pathologist-assisted training, did not yield great success in cTA ML classification of macrophages. The ability for a pathologist to classify all macrophages by eye was challenging, and the accuracy of the trained cTA ML classification was limited. However, using an immunofluorescence-guided approach, the cTA ML classification of macrophages was much more accurate.

Further refinement of the immunofluorescence-guided method presents opportunity for immune cell subset identification in the absence of subtype-specific IHC staining in the future.